XX IMEKO World Congress
Metrology for Green Growth
September 9–14, 2012, Busan, Republic of Korea

EVALUATION OF MACH NUMBER DISTRIBUTION AT THE TEST SECTION OF THE TTP TRANSONIC WIND TUNNEL

M. L. C. C. Reis[1], *J. B. P. Falcão Filho*[2], *B. Goffert*[3], *L. F. G. Moraes*[4]

[1,2,4] Instituto de Aeronáutica e Espaço, São José dos Campos, Brasil, Pr. Mal. Eduardo Gomes, 50, CEP 12228-904
[3] Instituto Tecnológico de Aeronáutica, São José dos Campos, Pr. Mal. Eduardo Gomes, 50, CEP 12228-901

Abstract: The distribution of the Mach number at the test section of the Brazilian Pilot Transonic Wind Tunnel is under evaluation for the subsonic, transonic and low supersonic ranges. The measured parameters in these investigative tests are static and total pressure of the airflow, which are the input quantities for the isentropic equation used for the Mach number estimation, which is the output quantity. The measurement of static pressures at several stations of the test section is accomplished by positioning a pressure probe at the centreline and by distributing pressure taps along the superior and inferior walls. The total pressure is measured at two locations: at the stilling chamber of the circuit and at the tip of the probe. Data reduction includes the evaluation of the uncertainties associated with the measured quantities, as well as their propagation to the output quantity, employing the Monte Carlo method. Least squares fitting is applied to the experimental data in order to supply Mach number distribution as a function of longitudinal positions of the test section. The distribution at the centreline resulting from the tests is compared to Computational Fluid Dynamics simulation for the supersonic regime.

Keywords: transonic wind tunnel, uncertainty in measurement, Monte Carlo method, Least squares fitting, CFD.

1. INTRODUCTION

Wind tunnels are experimental facilities designed to simulate flows encountered by aerospace vehicles during real flight. The metrological reliability of the data originating from wind tunnel tests depends on the knowledge of the quality of the flow in the test section of the aerodynamic circuit.

In order to investigate the Mach number distribution at the test section of the Brazilian Transonic Wind Tunnel Facility, a test campaign is being carried out to measure total and static pressures of the airflow. These two parameters are input quantities for the estimation of Mach numbers when employing isentropic relations [1]. To accomplish the investigation, a row of pressure taps was arranged on the superior and inferior walls of the test section and then connected to pressure measurement units. A pressure probe with static and total pressure ports was also employed.

One criterion to ensure a good quality of the flow is to periodically verify the standard deviation of the Mach number, σ_M, at the region of the test section where the test article is installed, known as the nominal test section [2]. The criterion for the standard deviation of the Mach number is $|2\sigma_M| \leq 0.001$.

Instead of the standard deviation parameter, this paper proposes the analysis of the flow quality through the evaluation of uncertainty in the Mach number, u_M. According to standard metrological recommendation, uncertainties associated with the experimental data are evaluated and propagated to the estimated Mach number [3].

2. THE TTP WIND TUNNEL

The Pilot Transonic Wind Tunnel, TTP, is located at the Aerodynamics Division of the Institute of Aeronautics and Space, Brazil (Fig. 1).

The tunnel is continuously driven by an 830 kW main axial compressor and can also be operated intermittently by means of an injection system, which supplies airflow for around 30 seconds. It is a variable-pressure wind tunnel with control capability to independently vary Mach number, stagnation pressure, stagnation temperature and humidity. The test section is 0.25 m high and 0.30 m wide and has longitudinally slotted walls to favor the uniformity of the airflow. At TTP, the Mach number range can vary from 0.20 to 1.3. Some configurations can be changed in order to allow better flow control such as reentry flaps position and the rate of forced mass extraction, determined by the Plenum Evacuation System, PES.

Fig. 1: The TTP aerodynamic facility.

A schematic picture of the aerodynamic circuit is presented in Fig. 2, highlighting its main parts: the axial compressor, cooler, stilling chamber, plenum chamber, high velocity diffuser and corners (numbered from 1 to 4). Arrows indicate the direction of the airflow. The test section, which receives the test article, is located inside the plenum chamber. Downstream of the stilling chamber one can see a convergent nozzle which characterizes subsonic and sonic flows at the test section. For supersonic regimes, the convergent nozzle must be replaced by a fixed geometry supersonic convergent-divergent nozzle.

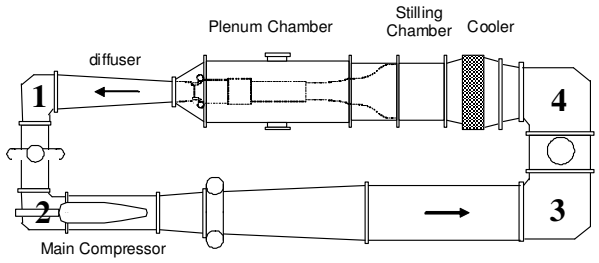

Figure 2: Schematic picture of the wind tunnel circuit.

A typical supersonic first throat is depicted in Fig. 3. Basically, at the convergent region, the subsonic flow accelerates to unitary Mach number at the smallest area of the nozzle, and is then accelerated again due to area expansion. Design of the best geometry must minimize the effects of expansion and compression waves originating between the initial and straightening regions which affects the flow uniformity at the test section.

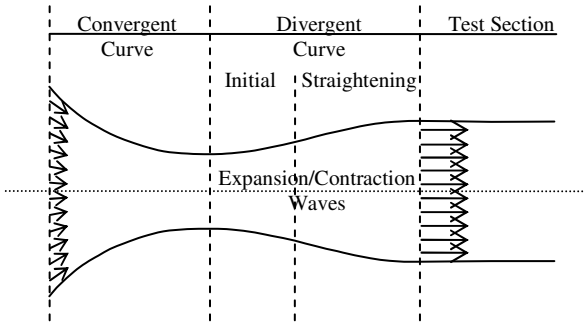

Figure 3: Supersonic convergent-divergent first throat scheme. Air flows from left to right.

3. METHODOLOGY

The Mach number, M, is the ratio of the flow velocity to the speed of sound. For compressible, isentropic flow, the Mach number can be expressed by [4]:

$$M^2 = \frac{2}{\gamma - 1}\left[\left(\frac{p_0}{p}\right)^{(\gamma-1)/\gamma} - 1\right] \qquad (1)$$

where
p_0: total pressure;
p: static pressure; and
γ: ratio between specific heats at constant pressure and constant volume. For air considered as a perfect gas, $\gamma = 1.4$.

The first step of the study was to analyze the central region of the test section. To estimate the ratio p_0/p, a pressure probe attached to a sting support was positioned at the centreline (Fig. 4). The probe has an ogive forebody, a main cylindrical body of 17.2 mm outer diameter and 1240 mm of length. Thirty three static pressure orifice stations with four orifices connected to a single pressure sensor at each station, and one total pressure tap at its tip, are used to make the measurements. Good accuracy is guaranteed with 0.5 mm diameter of the pressure taps holes. The probe wall thickness is 2.1 mm to ensure sufficient rigidity to avoid structural bending.

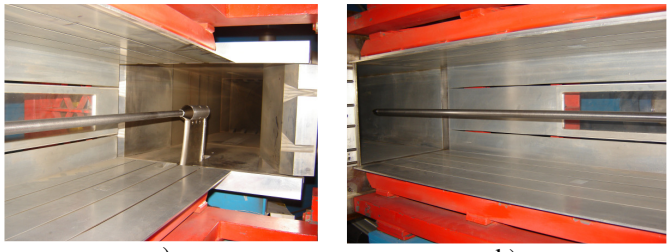

a) b)

Figure 4: Pressure probe installed in the test section. a) Attachment to the sting support. b) View upstream.

The second step was to analyze the TTP airflow behavior at regions near the walls. A row of thirteen pressure taps distributed along the ceiling (superior wall) and twelve along the floor (inferior wall) of the test section, connected to pressure instruments, were used for the static pressure measurements (Fig. 5).

The static pressure orifices are named A1 to A13 and B1 to B12 for the superior and inferior walls, respectively. The identification for the probe's thirty three static pressure orifices is C1 to C33 (Fig. 6).

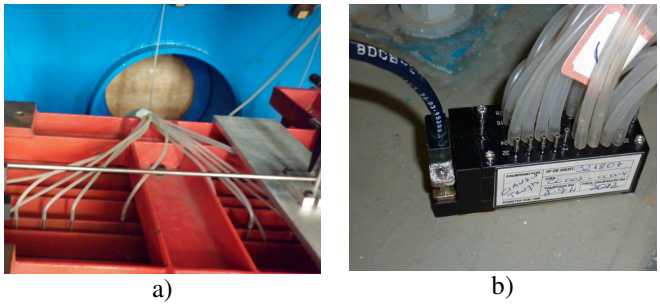

a) b)

Figure 5: a) Superior wall of the test section. b) Connection tubing to the pressure measurement instrumentation.

An instrument positioned before the test section, inside the stilling chamber, measures the total pressure. This measurement is necessary because the total pressure port of the probe will not measure correct values due to possible shock waves present in regimes superior to $M = 1.00$.

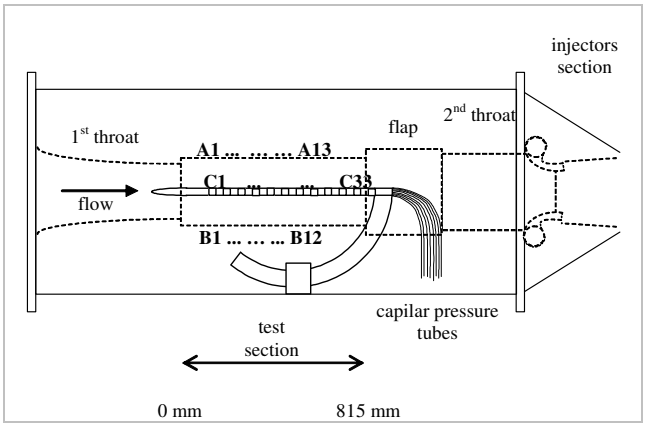

Figure 6: Pressure taps identification: **A** at superior wall, **B** at inferior wall and **C** at centre.

The mean value and standard deviation of the pressure signals, p_0 and p, supplied by the instruments during the runs of the wind tunnel tests are computed. This information is used to determine the probability density function for Mach numbers using the Monte Carlo method. The probability distributions for the input quantities are propagated through the mathematical model expressed by Eq. (1), resulting in the estimated M quantity and the standard uncertainty associated with this estimate, u_M [3]. The law of propagation of uncertainty could also had been used to assess Mach number uncertainty, but it was not chosen due to the inconvenience in providing the partial derivatives.

After evaluating the Mach number and associated uncertainty by the Monte Carlo method, curves of Mach number, M, as a function of the longitudinal position at the test section, x, are provided for all regimes covered by the tests. The least squares method is applied to each $M \times x$ curve, to supply calibration curves [4]. The fitting models are polynomials which have adjustable parameters a_j.

$$M = \sum_{j=0}^{n} a_j x^j \quad (3)$$

Initially, first degree polynomials are fitted to the data, i.e., $n = 1$ in Eq. (3).

The matrix design X are basis functions of the longitudinal position x and M is the vector composed by the values of Mach numbers estimated through the Monte Carlo method. The covariance matrix V of the output quantity is diagonal and its elements are the squared standard uncertainties also supplied by Monte Carlo. The linear regression results in the estimation of the vector a, composed of the polynomial parameters:

$$\hat{a} = \left(X^T \cdot V^{-1} \cdot X\right)^{-1} \cdot \left(X^T \cdot V^{-1} \cdot M\right) \quad (4)$$

where X^T is the transpose of matrix X, V is the covariance matrix and V^{-1} is the matrix inverse of V.

The matrix $\left(X^T \cdot V^{-1} \cdot X\right)^{-1}$ in Eq. (4) is called the error matrix because it contains information about uncertainties of the estimated parameters a. Its diagonal elements correspond to the variances and the off-diagonal elements are the co-variances of the fitted parameters.

The fitted Mach numbers, M_{fitted}, are estimated by:

$$M_{fitted} = X \cdot \hat{a} \quad (5)$$

The uncertainties associated with M_{fitted} are the positive square root of Eq. (6):

$$V_{M_{fitted}} = X \cdot V_{\hat{a}} \cdot X^T \quad (6)$$

where $V_{\hat{a}}$ is the error matrix $\left(X^T \cdot V^{-1} \cdot X\right)^{-1}$.

Quality of fitting is evaluated through the goodness-of-fit quantity, named chi-square [4]:

$$\chi^2 = \left(M - M_{fitted}\right)^T V^{-1} \left(M - M_{fitted}\right) \quad (7)$$

where M and M_{fitted} are Mach numbers estimated by Monte Carlo and least squares methods, respectively. The covariance matrix V is also a result of the Monte Carlo application.

4. RESULTS AND DISCUSSION

The uniformity of flow in transonic wind tunnels must be periodically verified to guarantee the metrological reliability of the tests performed in the installation.

The test campaign to analyse the Mach number distribution at the test section of transonic wind tunnel TTP considers nominal Mach numbers equal to 0.40, 0.60, 0.80, 1.00 and 1.30. A sonic nozzle was employed for the first four regimes whereas a supersonic convergent-divergent throat was employed for $M = 1.30$.

Ideally, the same Mach number value should be observed in any region of the test section. Although a uniform stream is extremely desirable in order to simulate real flight conditions, several sources of errors affect wind tunnel tests results. They are caused by instrumentation, wall interferences and other aerodynamic phenomena. Examples of aerodynamic effects are boundary layers on the test section surfaces, which affect the speed of flow, and the presence of shock waves beyond sonic regimes, which disturb flow properties.

An important contribution to the uncertainty associated to Mach number evaluation is the measurement precision of the pressure temporal acquisition, evaluated as a type A uncertainty. The dispersion of the pressure signal is, in part, due to the tunnel's control system, which is not capable of supplying a more stable flow.

Figures 7 and 8 illustrate the plot of static pressures as a function of time for nominal Mach numbers 0.60 and 1.30, respectively. Only results from ports belonging to the nominal test section region are shown: A7 to A12, B7 to B12 and C14 to C29. Estimated Mach numbers are reported in relation to the position of each of these ports. Port C21 did not work properly below supersonic regimes and its

measured values were only considered in data reduction for $M = 1.30$.

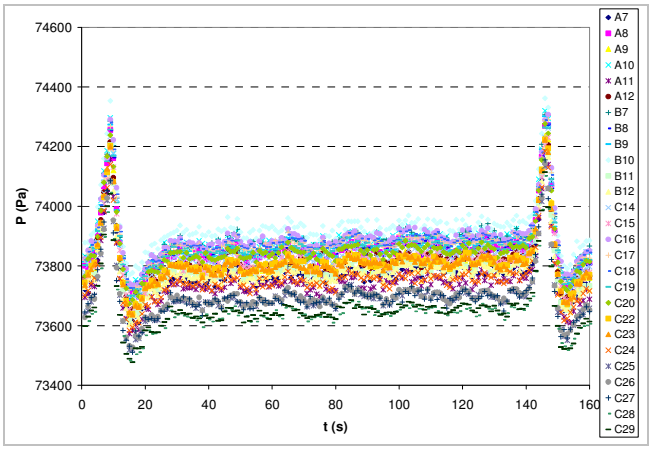

Figure 7: Static pressure measurement at inferior and superior walls and at the probe, $M = 0.60$.

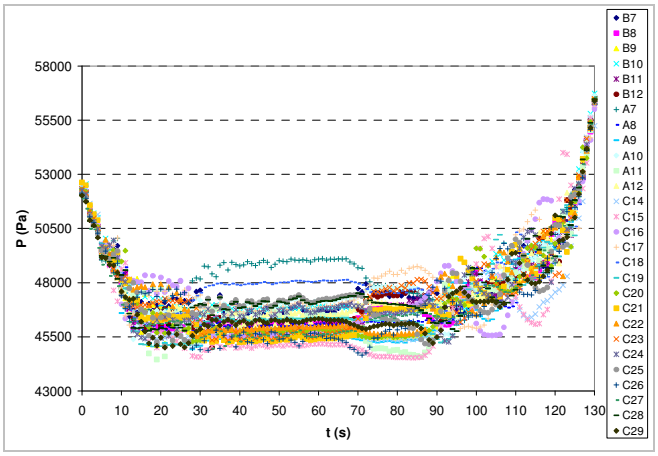

Figure 8: Static pressure measurement at inferior and superior walls and at the probe, $M = 1.30$, PES max.

When the desired regime settles down, an interval of the pressure signals is chosen and the average and standard deviation are calculated. The same procedure is performed for total pressure and the ratio p_0/p of average values of total and static pressures is computed. This ratio is included in Eq. (1) to supply the Mach number values in each nominal test section station.

For $M = 0.60$, the interval 90 to 135 s between two signal transients was chosen (Fig. 7). The transient is caused by the wind tunnel drier system, which controls the humidity of the airflow. For the $M = 1.30$ regime, the main compressor plus injection system is employed to accelerate the flow. The plenum evacuation system, PES, was set at maximum rate, which corresponds to a value of 1.9 % of the test section mass flow. In Fig. 8, the chosen interval corresponds to 40-60 s. The disturbance outside this interval is due to the activation of the injection system. The transient occurs because the injection is either being activated or is losing power.

Figure 9 shows the results of applying Eq. (1) for M equal to 0.40, 1.00 and 1.30. For clarity, the results were divided by the nominal Mach numbers. Static and total pressures are measured by the probe, therefore the shown data are related to the test section centreline. Pressure tap C1 is on the left and pressure C33 is on the right of the figure. Positions are related to the pressure tap distance from the test section entrance.

One can note in Fig. 9 that in the subsonic range, $M = 0.40$, the Mach number profile shows uniformity to a certain extent, with a moderate positive gradient in the downstream direction, dipping as one reaches the end of the test section. There is a flow disturbance at the beginning of the test section as well. Results for M equal to 0.60 and 0.80 are not shown in Fig. 9, but they have the same behaviour as $M = 0.40$. In the sonic range ($M = 1.00$), before going down at the end of the test section, the signal increases. For nominal $M = 1.30$, the dispersion of estimated Mach numbers throughout the test section is greater than in the other lower regimes. This behaviour is also observed in other wind tunnel facilities [5].

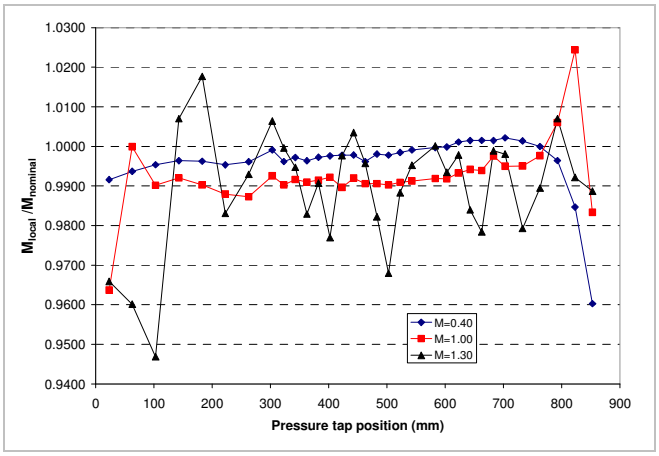

Figure 9: Mach number distribution at test section centreline.

Figure 10 presents the set of results at the centreline for all Mach numbers covered in the tests. In this picture, the shadowed region represents the nominal test section, which starts at 423 mm and ends at 733 mm. The dashed vertical line marks the end of the test section, which is a total of 853 mm.

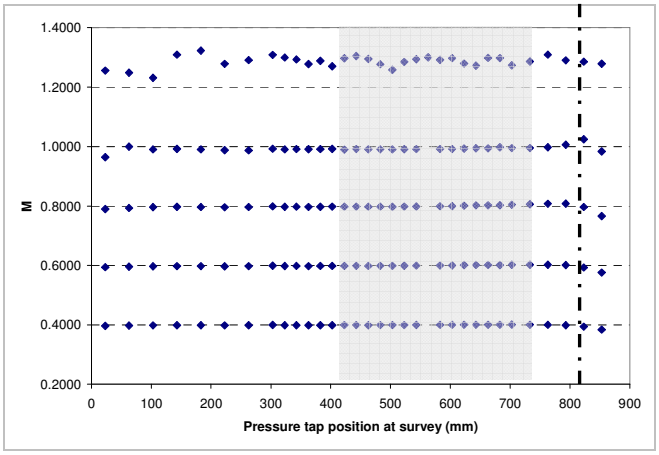

Figure 10: Mach number centreline distribution in the pressure probe measuring stations.

Mach number uniformity results for the nominal test section centreline and superior and inferior walls are plotted together in Fig. 11. Superior taps are aligned to the inferior ones and are located at 434, 481, 503, 552, 578 and 641 mm from the test section entrance. Most of the probe pressure tap locations do not coincide with the positions of the taps on the walls. The C14 to C29 positions are 423, 443, 463, 483, 503, 523, 543, 563,583, 603, 623, 643, 663, 683, 703 and 733 mm. There are no significant discrepancies in data in general, but some divergences occur for M = 1.30.

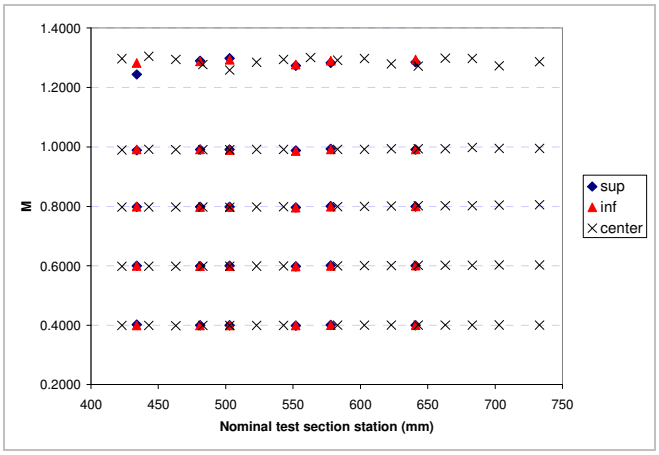

Figure 11: Mach number data for centreline and superior and inferior walls at the nominal test section.

Tests at M = 1.30 were conducted with the supersonic nozzle. A Computational Fluid Dynamics simulation, CFD, employing Euler equations in 2D analysis was performed to preview the Mach number distribution expected at the test section (Fig. 12) [6, 7]. Position x = 0.0 m marks the beginning of the test section. The supersonic nozzle is depicted in the negative part of axis x. The probe inside the test section was not considered in the simulation.

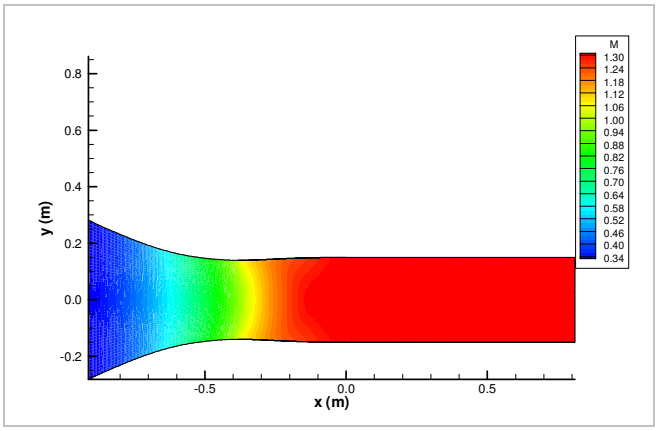

Figure 12: Result of numerical simulation for Mach number output at centreline. Supersonic nozzle.

According to the simulation, the average and standard deviation of the expected Mach number in the nominal test section was 1.3014 and 0.0013, respectively, with a difference between the maximum and minimum values equal to 0.0038. These simulating values are compared to experimental data in Fig. 13. Note that simulated and experimental data do not comply. For the test results, the average Mach number value is 1.3043, the standard deviation is 0.0106, which is ten times greater than the simulated data, and the difference is 0.0402. The oscillation in the simulated curve corresponds to disturbances caused by the formation of expanding and compressing waves at the nozzle. In an ideal nozzle design such a disturbance would not appear because the expanding and compressing waves would cancel each other out [1]. Reasons for the dispersion of experimental data are not completely understood, but the instrumentation is probably capturing compression and expansion wave interactions.

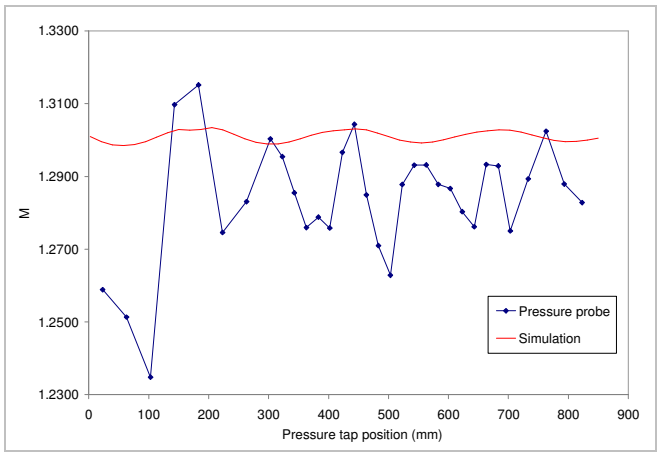

Figure 13: Supersonic Mach number comparison between CFD simulation and experimental data.

To analyse to what extent the presence of the probe would increment the dispersion in the supersonic regime, tests were conducted with and without the probe inside the test section. Figure 14 shows the simulated values at the centreline and the experimental values at the top wall. The standard deviation with and without the probe are of the same order, 0.0137 and 0.0154 respectively, indicating that disturbances have other origins.

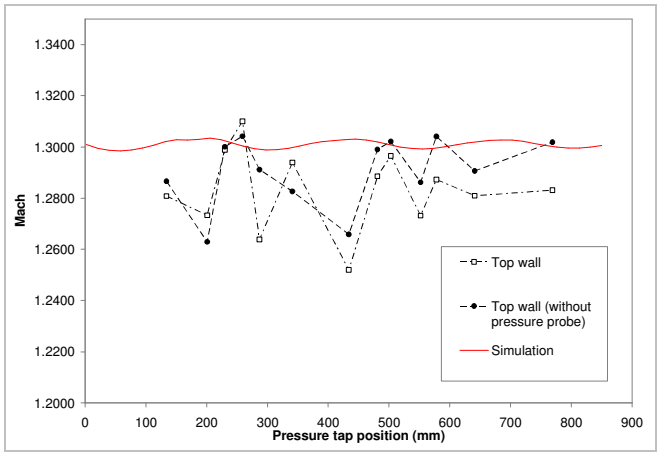

Figure 14: Withdrawing the probe does not reduce experimental Mach number dispersion.

Besides providing Mach numbers, M, estimated through Eq. (1), this study also supplies Mach number calibration

curves and associated uncertainties, u_M, for all airflow regimes covered in the tests.

The Monte Carlo method was used to obtain u_M. Probability distributions characterized by the mean and standard deviations calculated from pressure signal were propagated through Eq. (1) to estimate the probability distribution for the output quantity M. Data reduction included all nominal test section stations. Codes in MATLAB® were elaborated to accomplish this task. The selected number of trials was 5,000.

Once the code computes M and u_M values, least squares fitting is employed to the data (x, M), for Mach number equal to 0.40, 0.60, 0.80, 1.00 and 1.30. The results at the centerline are shown in Table 1. The fitted curves are first degree polynomials. Only data originating from the nominal test section were considered in the regression.

The quality of the fitting was verified through the chi-square quantity, Eq. (7). An indication of a good fit is χ^2 typically close to the number of degrees of freedom, ν, which corresponds to the difference between the number of data points and the number of parameters a in Eq. (3) to be fitted. There are 16 data points for M = 1.30 and 15 for the other regimes therefore, ν is equal to 14 for the former and 13 for the latter airflow regimes.

Table 1: Calibration curves for nominal Mach numbers and corresponding quality of fit.

M	1st degree fitting	χ^2	χ^2_ν
0.40	$0.3958(5) + 70(9)\times10^{-7}\,x$	16	1
0.60	$0.5912(9) + 54(16)\times10^{-7}\,x$	19	1
0.80	$0.7851(10) + 261(18)\times10^{-7}\,x$	40	3
1.00	$0.9825(5) + 170(9)\times10^{-7}\,x$	77	6
1.30	$1.3045(23) - 28(4)\times10^{-6}\,x$	1020	73

The least squares regression slope dM/dx should be as close to zero as possible to indicate a gradient-free test section. A gradient different from zero indicates that the axially slotted top and bottom walls were not capable of eliminating the downstream boundary layer thickness growing at the test section end region. According to Table 1, slope values are positive for M up to 1.00 and negative for 1.30. A possible explanation for this opposite behavior could be that a decreasing area caused by the effect of the boundary layer growth at the walls and at the probe would result in an accelerated flow for subsonic regimes and a decelerated flow for supersonic regimes.

One way to minimize the boundary layer effect is to change the configuration of the Plenum Evacuation System, PES. This system allows forced mass extraction in the plenum chamber to modify the mass flow through the walls in order to obtain the best condition for a particular test article installed in the test section. Some tests with the probe were conducted for M = 0.80 to analyze the effectiveness in reducing the gradient by changing the rate of forced mass extraction. Figure 15 presents the Mach number distribution for PES set for extracting mass at rates 0, 1.0, 1.5, 2.0, 2.5 and 2.8 %. Better results are achieved for 2.8 %, which presents a reduction in the slope of approximately 2.6×10^{-5}, as indicated in Table 1, to 1.5×10^{-5}.

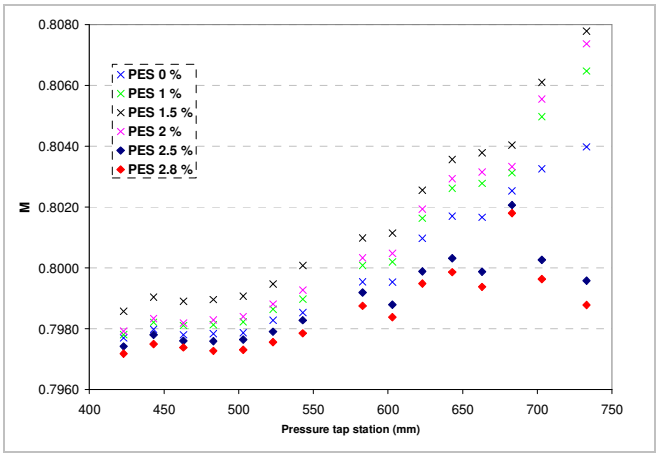

Figure 15: Forced mass extraction effect on airflow gradient.

The last column in Table 1 presents the ratio between the chi-square and the degrees of freedom, known as reduced chi-square, χ^2_ν. A value equal to 1 for the reduced chi-square is expected if the fitting function agrees with the data. One can see in Table 1 that only the fittings for M equal to 0.40 and 0.60 meet this criterion, indicating that either the assumed model is not appropriate or the data point uncertainties were underestimated [4].

A different model was chosen to fit Mach number 0.80 data in an attempt to improve the fitting results. When the polynomial degree is increased from 1 to 3, the χ^2 quantity improved to 15, compared with the value 40 presented in Table 1. The comparison between the first and third degree polynomial for M = 0.80 can be seen in Figs. 16 and 17. Fitted points represent M values estimated by the Monte Carlo method, solid lines represent fitted curves and dashed lines represent superior and inferior uncertainty limits.

The same procedure was performed for M = 1.00 and 1.30 but results indicated that changing the polynomial degree is not sufficient to achieve a good fit.

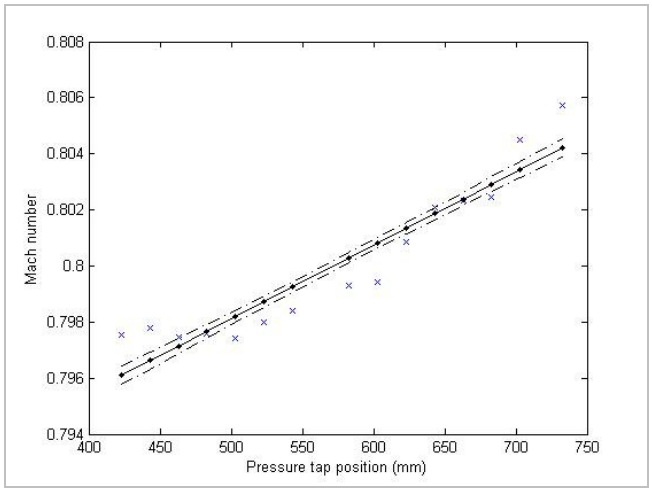

Figure 16: Least squares fit to a first degree polynomial.

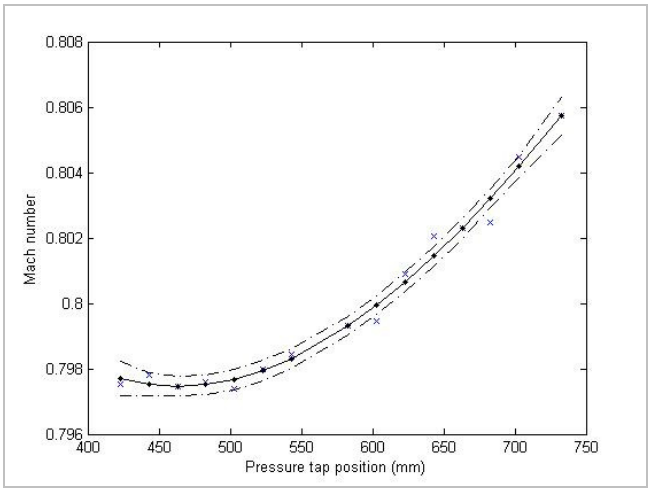

Figure 17: Least squares fit to a third degree polynomial.

4. CONCLUSIONS

In order to verify the quality of the airflow of the TTP wind tunnel, the Mach number distribution at the test section was analyzed.

Tests included investigation at the floor and ceiling walls and at the central region of the test section.

Calibration curves $M \times x$ relating Mach number and position were presented for flow regimes equal to 0.40, 0.60, 0.80 1.00 and 1.30. Uncertainty limits were also supplied for the curves, taking into account uncertainties in the measured pressures, which propagate to Mach numbers.

The calibration curves can be employed to correct Mach numbers obtained during wind tunnel tests and can be used for comparisons with future studies of TTP flow uniformity.

The least squares method has failed to fit sonic and supersonic data, indicating that additional studies must be carried out at TTP for regimes greater than $M = 1.00$.

5. REFERENCES

[1] J. D. Anderson J., Fundamentals of Aerodynamics, 3rd ed., 2001.

[2] M. W. Davis, J. A. Gunn, R. D. Herron, E. M. Kraft, Optimum Transonic Wind Tunnel", in Proc. of AIAA 14th Aerodynamic Testing Conference, AIAA-86-0756-CP, West Palm Beach, 1986.

[3] JCGM 101, Evaluation of measurement data – Supplement 1 to the "Guide to the expression of uncertainty in measurement"- Propagation of distributions using a Monte Carlo method, 2008.

[4] W. H. Press, S. A. Teukolsky, W. T. Vetterling, B. P. Flannery, Numerical Recipes, Cambridge University Press, 2nd ed.,1992.

[5] R. L. Parker Jr., Flow Generation Properties of Five Transonic Wind Tunnel Test Sections Wall Configurations, AEDC-TR-75-73, Aug. 1975.

[6] B. Goffert, G. P. A. Ubertini, J. B. P. Falcão Filho, Design of a Supersonic First-Throat for a Transonic Wind Tunnel and Numerical Evaluation, in Proc. of 21st Brazilian Congress of Mechanical Engineering, 2011.

[7] J. D. Anderson J., Computational Fluid Dynamics: the Basics with Applications, McGraw-Hill Inc., 1995.